DOI: 10.22607/IJACS.2017.503004

Available online at
www.ijacskros.com

Indian
Journal of Advances in
Chemical Science

Indian Journal of Advances in Chemical Science 5(3) (2017) 137-141

Synthesis and Characterization of Zinc Oxide Nanoparticles by Solution Combustion Method: DC Conductivity Studies

D. Syamala Bai[1], V. Ramesh Kumar[2], R. Padma Suvarna[1]

[1]Department of Physics, JNTUA, Anantapur, Andhra Pradesh, India. [2]Department of Physics, Government Degree College, Pattikonda, Kurnool, Andhra Pradesh, India.

Received 19th April 2017; Revised 15th May 2017; Accepted 25th May 2017

ABSTRACT

Zinc oxide nanoparticles were synthesized via low temperature solution combustion method with using different fuels (glycine, citric acid, urea, and raphanus sativus [radish] extract). The particles obtained were well characterized by powder X-ray diffraction and field emission scanning electron microscopy images. DC conductivity studies were performed in the temperature range 320-385 K.

Key words: *Solution combustion synthesis, Powder X-ray diffraction, Field emission scanning electron microscopy, Raphanus sativus, DC conductivity.*

1. INTRODUCTION

Oxide based electronics have been sound established as an substitute to silicon technology, however, typical processing requires complex, and high-vacuum equipment, which is a major drawback, particularly when targeting low-cost applications. The opportunity to deposit the materials by low-cost techniques such as inkjet printing has drawn incredible interest in solution-processible materials for electronic applications, nevertheless, high processing temperatures still required. To overcome this issue solution combustion synthesis (SCS) has been recently pursued. Taking improvement of the exothermic nature of the reaction as a source of energy for localized heating, the precursor solutions can be converted into oxides at lower processing temperatures. This can be applied to any metal ions to produce the desired oxide, opening unlimited potential to materials composition and combinations. SCS has been applied for the production of semiconductor thin films based on zinc oxide (ZnO), In_2O_3, and SNO_2 and combustion of these oxides and also for high K dielectrics such as Al_2O_3 [1]. ZnO nanoparticles are used in various commercial products such as sunscreens, cosmetics, and gas sensors and the areas of antibacterial activity and photocatalysis [2]. The increase in the DC conductivity of ZnO nanoparticles as well as nanocomposites of polyaniline/ZnO shows the semiconducting behavior [3].

Depending on the type of the precursor and also on the conditions of the process organized, the SCS may occur as either volume or layer-by-layer propagating combustion modes. This process not only yields nanosize oxide materials but also allows uniform (homogeneous) doping of trace amounts of rare earth impurity ions in a single step. Among the gamut of papers published in recent years of SCS, synthesis of luminescent materials and catalysts occupy the lion share. The synthesis of nanophosphors is currently a hot topic in the field of combustion synthesis by utilizing fuels such as hexamine, urea, glycine, ammonium nitrate, citric acid, sucrose, urea mixed with boric acid flux, oxalyldihydrazide (ODH), and thiourea. The year 2008 is a landmark year in SCS marking two decades of the first publication on SCS of alumina and related oxides. Patent on synthesis of MgO and ZnO for defluoridation and arsenic removal has also been field [4].

With glycine fuel, combustion is an explosive kind with no flame but results into high surface area dry powder with soft agglomerations [5,6].

Citric acid as fuel gives a higher number of moles of gases compared to glycine during combustion which improves the surface area. The parameters that affect the powder properties are oxidant to fuel ratio. The fuel should be added in such a way that the metal nitrate to fuel ratio should be maintained at the molecular level. The oxidant to fuel ratio should be varied from fuel deficient to fuel rich to study the type of propagation

*Corresponding Author:
E-mail: dsyamala17@gmail.com

of SCS and powder properties. The precursor should give an intimate blending of the starting constituents preventing the random redox reaction between a fuel and nitrates. The oxidant to fuel ratio φ can be the ratio of oxidizing valency to reducing valency. If φ is less than one, the ratio is fuel deficient, fuel rich if φ is greater than one and it is stoichiometric if φ is equal to one, quantifying the quantity of oxygen in excess deficient or appropriate. With oxidant to fuel ratio varying from 1:1.1 to 1:1.9 gradually, it is observed that the surface area increases from 39.58 to 118.03 m^2/g. With an average size of the agglomeration changing from 4.67 to 13.42 μm [7].

Hydrazine based fuels such as carbohydrazide, ODH, and malonic dihydrazide are combustible due to the presence of N-N bond that decomposes exothermically to N_2 (N≡) were found to be appropriate. Some of the purposes of the fuels are 1. Liberation of CO_2, H_2O and heat after combustion as fuels are the sources of C and H 2. Formation of the complex with the metal ions that results in homogeneous mixing of cations in solution 3. Breakdown of components from which they are formed. Some of the characteristics of ideal fuel are:

- Have low ignition temperature (<500°C)
- Soluble in water
- Compatible with metal nitrates
- Evolve large amounts of gases
- Harmless during combustion
- Readily available or easy to prepare.

Particle size of the combustion product can be controlled by the slow rate of burning, exothermicity reduction, more number of release of gaseous products, and linear combustion instead of volume combustion [8].

2. EXPERIMENTAL

2.1. Materials

Zinc nitrate ($Zn(NO_3)_2$ $6H_2O$), glycine ($C_2H_5NO_2$), citric acid (C_6H_8O7), urea (NH_2CONH_2), ammonium hydroxide, nitric acid, and raphanus sativus (radish) solution of analytical grade were used.

2.2. Preparation

The synthesis process involves the combustion of redox mixtures in which zinc nitrate ($Zn(NO_3)_2$,$6H_2O$) acted as an oxidizing reactant and glycine as a reducing one. All the reagents were of analytical purity and used without further purification. Zinc nitrate and raphanus sativus solution are mixed with a minimum quantity of double distilled water in a cylindrical Petri dish and stirred for few minutes until a clear solution was formed. The dish is introduced into a muffle furnace maintained at 300°C. The solution initially undergoes dehydration, followed by decomposition with the evolution of large amounts of gases. The mixture then froths and swells forming foam, which ruptures with a flame and glows to incandescence. During incandescence, the foam further swells to the capacity of the container. The entire combustion process gets over in 7-8 min. The foam is grinded to obtain fine powder of ZnO. The entire process is repeated to prepare ZnO nanoparticles using different fuels, citric acid, and urea and the solution of raphanus sativus (green fuel) instead of glycine.

2.3. Characterization

X-ray diffractograms were obtained using powder X-ray diffraction (PXRD) Goniometer with CuK_α radiation. The scanning electron microscope (SEM) images were taken by SEM Zeiss Supra 40 VP. The low-temperature electrical conductivity measurements were done in Janis liquid helium cryostat connected to Lakeshore temperature controller, Keithley 2000 multimeter, and Keithley 220 current source.

2.4. DC Conductivity of ZnO Nanoparticles Experiment

The apparatus used shown in Figure 1 for the DC conductivity measurement consists of four probe arrangement, sample, measuring unit containing oven, controller, constant current generator, and multi-range digital voltmeter.

Put the sample on the base plate of the probe arrangement, apply pressure gently and place it in the oven. Connect the outer pair of the leads to the constant current power supply and the inner pairs to the voltage terminals. When the digital panel meter kept in this measuring unit, the light emitting diodes glows and the voltage can be noted. Increase the temperature in steps from 320 to 385 K and take the corresponding voltage readings [9].

3. RESULTS AND DISCUSSIONS

3.1. PXRD Analysis

Figure 2 shows the PXRD of as formed ZnO samples. The three strongest XRD peaks for ZnO are detected with Miller indices (100), (002), and (101) corresponding to Bragg angles 31.8, 34.5, and 36.4°,

Figure 1: Experimental set- up of DC conductivity measurement.

respectively. The other diffraction peaks are observed at (102), (110), (103), and (112). All diffraction peaks can be readily indexed to wurtzite hexagonal ZnO structure with lattice constants a=3.2511(1) Å and c=5.2076(2) Å, consistent with the standard PDF database (JCPDS file No. 36-1451). The characteristic peaks are higher in intensity which indicates that the products are of good crystalline nature. No peaks corresponding to impurities are detected, showing that the final product is purely ZnO. The peak list of ZnO nanoparticles shows that the full width at half maxima (FWHM) of major peaks decreases and confirms the grain size growth. The average crystallite size is estimated from the Debye–Scherrer's equation:

$$D = \frac{k\lambda}{\beta \cos\theta}$$

Where β is FWHM (rad), λ is wavelength of X-rays, θ is diffraction angle. The average crystallite size (D) is found to be in the range 28.49 nm. The surface area of synthesized ZnO nanoparticles was found to be 37.56 m^2/g.

Total surface area=6000/D ρ, where D is the density of the NiO nanoparticles, ρ is the diameter of the nanoparticle.

The wurtzite structure is non-centrosymmetric, that is, lack of inversion symmetry. Due to this wurtzite structure crystals generally exhibit properties such as piezoelectricity and pyroelectricity, which centrosymmetric crystals lack. This structure is a member of the hexagonal crystal system and consists of tetrahedrally coordinated zinc and oxygen atoms that are stacked in an ABBABBABB pattern. The unit cell parameters of wurtzite are a=b=3.82A°=382 pm, c=6.26A°=626 pm, V=79.11A°, Z=2.7 [10].

3.2. Field Emission SEM (FESEM) Analysis

The FESEM images of synthesized ZnO nanoparticles shown in Figure 3 represent the wurtzite structure. These pictures confirm the

Table 1: Variation of voltage (V) with absolute temperature (T)

T	V	ρ	$1/T*10^{-3}$	Log ρ
320	49.7	15.1	3.125	1.18
325	43.8	13.31	3.076	1.12
330	39.1	11.88	3.030	1.07
335	35.0	10.64	2.985	1.02
340	30.4	9.24	2.941	0.96
345	26.2	7.96	2.898	0.90
350	22.6	6.87	2.857	0.83
355	19.2	5.83	2.816	0.76
360	16.5	5.03	2.477	0.70
365	14.2	4.31	2.739	0.63
370	12.2	3.70	2.702	0.56
375	10.6	3.22	2.666	0.50
380	9.2	2.79	2.631	0.44
385	7.9	2.40	2.597	0.38

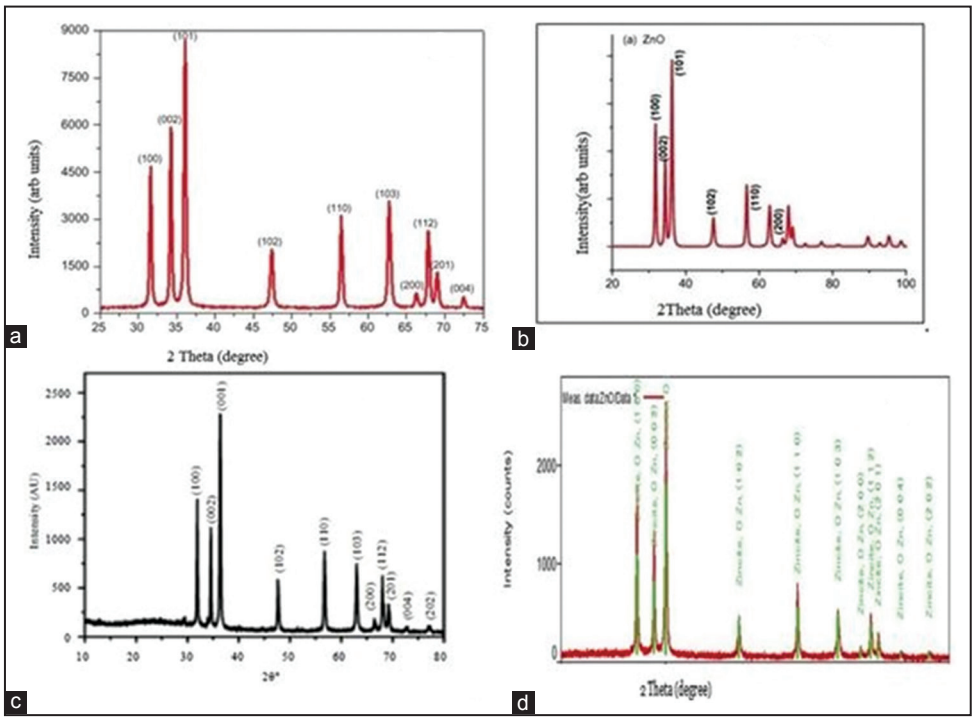

Figure 2: Powder X-ray diffraction (a) with glycine as fuel, (b) with citric acid as fuel, (c) with urea as fuel, and (d) with raphanus sativus as fuel.

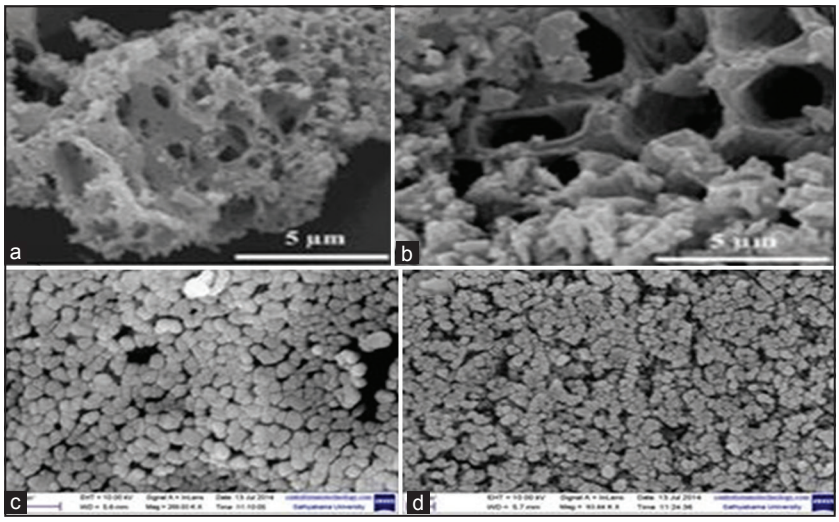

Figure 3: Field emission scanning electron microscopy images of zinc oxide nanoparticles (a) with glycine as fuel (b) with citric acid as fuel (c) with urea as fuel and (d) with raphanus sativus as fuel.

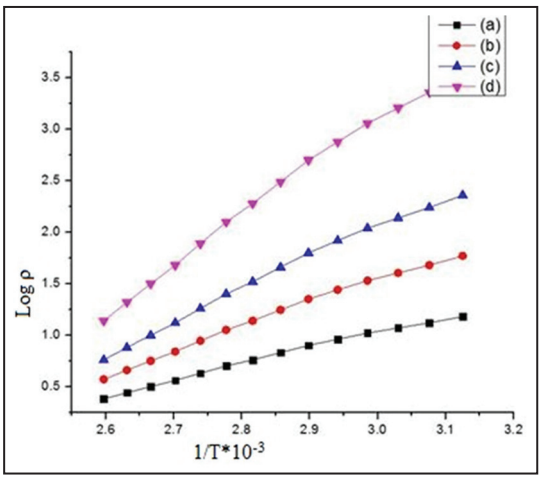

Figure 4: DC conductivity studies of zinc oxide nanoparticles (a) with glycine as fuel, (b) with citric acid as fuel, (c) with urea as fuel, and (d) with raphanus sativus as fuel.

formation of ZnO nanoparticles. These pictures substantiate the approximate spherical shape to the nanoparticles, and most of the particles exhibit some agglomeration. From the pictures, it is also seen that the size of the nanoparticle is more than that calculated from the Debye-Scherrer formula indicating the agglomeration of crystallites in ZnO nanoparticles. The aggregation of particles should have been originated from the large specific surface area and high surface energy of ZnO nanoparticles. The aggregations might have occurred probably during the process of drying. It is observed that the concentration of plant extract does not affect nanostructure of ZnO. The average grain size is calculated by the formula G_a=1.5L/MN where L is the average of the test lines drawn on the FESEM image, N is the average number of grains intersecting the test line, M is the magnification of the FESEM image. It is found that the average grain size is 50 nm [11].

From Figure 4 and Table 1, graph drawn between the reciprocal of temperature and logarithmic value of resistivity shows the semiconducting behavior of ZnO nanoparticles.

4. CONCLUSION

ZnO nanoparticles were successfully prepared through SCS with fuels glycine, citric acid, urea, and raphanus sativus extract and were characterized through PXRD and FESEM. The PXRD spectra and FESEM images of the samples do not show any appreciable difference or change of the sample properties. The DC conductivity studies showed semiconducting nature of the ZnO nanoparticles.

5. REFERENCES

1. R. Branquinnho, A. Santa, E. Carlos, (2016) SCS: Appltiicaons in oxide electronics. In: ***Developments in Combustion Technology***, Croatia: InTech.
2. D. Nohavica, P. Gladkov, (2010) ZnO nanoparticles and their applications - New achievements. ***Proceedings of the 2nd International Conference on Nanotechnology (NANOCON'10),*** Colomouc, Czeh Republic, EU.
3. G. K. Vinayak, S. B. Chakradhar, M. V. N. Prasad, (2015) Synthesis, characterization and DC conductivity studies on polyaniline/ZnO nanocomposites, ***Ferroelectrics***, **486:** 106-113.
4. S. T. Aruna, A. S. Mukasyan, (2008) Combustion synthesis and nano materials, ***Current Opinion in Solid State and Material Science***, **12:** 44-50.
5. B. Abasht, S. M. Mirkazemi, A. Beitollahi, (2017) Solution combustion synthesis of ca hexaferrite using glycine fuel, ***Journal of Alluys and compounds,*** **708:** 337-343.

6. A. C. Luicilha, R. Afonso, P. R. C. Silva, (2014) ZnO prepared by solution combustion synthesis, characterization and application as photoanode, ***Journal of the Brazilian Chemical Society***, **25:** 1091-1100.
7. J. Kers, P. Kulu, A. Arunitt, (2010) Determination of physical, mechanical and burning characteristics of polymeric waste material briquettes, ***Estonian Journal of Engineering,*** **16:** 307-316.
8. T. Theivasanthi, M. Alagar, (2010) X-Ray diffraction studies of copper, nanopowder, ***Archieves of Physics Research,*** **1:** 112-117.
9. M. A. Bilya, M. Hasssan, (2016) Determination of band gap of a semiconductor, Germanium chip using four probe set up, ***International Journal of Science and Research***, **5:** 1137-1140.
10. L. D. Jadhav, S. P. Patil, A. P. Jamale, (2013) Solution combustion synthesis: Role of oxidant to fuel ratio on powder properties, ***Material Science Forum***, **757:** 85-98.
11. H. Sarma, D. Chakrabortty, K. C. Sarma, (2014) Structural and optical properties of Zno nanoparticles, ***IOSR Journal of Applied Physics***, **6:** 8-12.

****Bibliographical Sketch***

D. Syamala Bai did her MSc., MPhil., Physics in SK University, Anantapur. Now she is PhD research scholar in JNTUA, Anantapur. She presented her research papers in International Conferences conducted by IISC Bengaluru, RVCE, Bengaluru, Shivaji University, Kolhapur, Nagarjuna University, Guntur, MG University, Kottayam and in National Conferences conducted by JNTUH, Hyderabad and Govt. College (M) UG and PG, Anantapur.